# FAILURE OF STEEL ANGLES UNDER VERY LOW CYCLES OF LOADING

○Yeon-Soo Park, Graduate Student in Civil Engineering, Kyoto University
Satoshi Iwai, Research Associate, Disas. Prev. Res. Inst., Kyoto University
Hiroyuki Kameda, Professor, Disas. Prev. Res. Inst., Kyoto University
Taijiro Nonaka, Professor, Disas. Prev. Res. Inst., Kyoto University

1. INTRODUCTION The main objective of this study is to clarify the quantitative relationships among the important physical factors associated with failure of steel members under strong seismic excitations through very low-cycle fatigue tests. Very low-cycle fatigue is herein meant to be structural fatigue causing cracks and rupture in the course of loading repetitions of the order of a few to twenty cycles. The previous research[1)] showed that initiation of cracking due to very low-cycle loading is closely related to residual local strain of the order of 25-40%, regardless of loading patterns, failure modes, and width-to-thickness ratios. This experimental study is focusing on effects of slenderness ratio of angles and loading sequence on failure behavior.

2. TEST PROGRAM The test specimens were angles L-40x40x3 and L-40x40x5 of SS41 grade. The yield stress and the ultimate tensile strength of the materials were ranged within 339-371 $N/mm^2$ and 449-469 $N/mm^2$, respectively. A total of 20 specimens was tested. Each specimen was pin-supported at both ends. The effective length $l$ of the tested part was 318mm (or 300mm) or 618mm as indicated in Table 1. Test parameters are summarized as follows: 1) slenderness ratio $\lambda$, 2) width-to-thickness ratio $b/t$, 3) loading pattern, and 4) deflection mode. Loading was controlled by the relative axial displacement $\Delta$ in the contraction side, programmed as in Fig. 1.

3. EFFECTS OF SLENDERNESS RATIO AND WIDTH-TO-THICKNESS RATIO During testing, the global buckling deformation was accompanied by local buckling of the plates of the leg at the mid-part of the specimen. No torsional deformation was observed in the L5 series of specimens, but occurred in both L3 and H3 series. These phenomena were obviously found in the H3 series which was more slender than the L3 series. Nine specimens, for which the value $f_{rup}$ is indicated in Table 1, were completely ruptured within the programmed loading cycles. The test results show that $f_{rup}$ decreases as $b/t$ becomes smaller and $\lambda$ becomes larger. This may be because the local deformation of the angle was severely concentrated in these cases. However, regardless of the values of $b/t$ and $\lambda$, the maximum absolute values of residual "net" strains in a cracked portion, excluding contributions from the crack opening, of all the specimens were in the range of 25-35% on the elongation side and 30-40% on the contraction side (see $\varepsilon_{tens}$ and $\varepsilon_{comp}$ in Table 1).

4. ENERGY DISSIPATION BEHAVIOR The relationships between the dissipated energy $E$ and the number of cycles $f$ are shown in Fig. 2 for all the specimens, where $E_o$ is the maximum elastic strain energy which can be stored in the tested part of the specimen. In the cases of the same loading pattern and the same deflection mode, very similar processes of energy dissipation were observed (see curves for $L5CP_a$ and $L5CP_b$, and $L3CP_a$ and $L3CP_b$ in Fig. 2(b)). If deflection modes are different, however, cumulative energy dissipation behavior is quite different even among specimens under the same loading pattern (see (a), (b) and compare (c) with (d) in Fig. 2). From comparison of three types of loading patterns, C, G and S, effects of loading sequence are investigated. In the case of the positive deflection mode (see Figs. 2(c) and (e)), the number of cycles at rupture $f_{rup}$ becomes small in the order of the C, G and S types of loading. But the energy dissipation capacity is not significantly different among these three types. Thus, the stepwise displacement amplitude loading shown in Figs. 1 (c) and (d) resulted in similar amounts of damage.

5. CONCLUSIONS Based on this experimental study the following conclusions are obtained.
1) The number of load cycles at rupture decreases as width-to-thickness ratio becomes smaller and slenderness ratio becomes larger, because of severe concentration of local deformation in angles.
2) Residual strains at the outbreak of a visible crack under very low-cycle loading were of the order of 25-40%, regardless of loading patterns, deflection modes, slenderness ratios and width-to-thickness ratios.
3) Energy dissipation capacity depends heavily on the entire history of loading, failure.modes,

slenderness ratios and width-to-thickness ratios.

4) The number of cycles at rupture $f_{rup}$ becomes small in the order of the C, G and S types of loading.

6. REFERENCE 1) Y.-S. Park, S. Iwai, H. Kameda and T. Nonaka : Very Low Cycle Fatigue Testing of Steel Angles for Earthquake Loading, Proc. of The Annual Conference of Kansai Chapter of JSCE , Vol. 1, pp.I-50-51, 1991.

Table 1 Test parameters and results.

| Specimen Name | Length $l$ (mm) | Slenderness ratio $\lambda$ | Width-to-thickness ratio $b/t$ | Loading pattern | Deflection mode | Crack $f_{cav}$ | Number of load cycles Crack $f_{vex}$ | Crack $f_{pen}$ | Rupture $f_{rup}$ | Dissipated energy $E/E_o$ | Strain at cracked portion Tens. $\varepsilon_{tens}$(%) | Comp. $\varepsilon_{comp}$(%) |
|---|---|---|---|---|---|---|---|---|---|---|---|---|
| L3IP | 318 | 40.5 | 14.1 | I | P | 17 | 18 | 18 | -- | 131 | -- | -- |
| L3IN | 301 | 37.4 | 15.8 | I | N | 20 | 21 | 21 | -- | 235 | -- | -- |
| $L3CP_a$ | 300 | 37.3 | 15.8 | C | P | 9 | 10 | 10 | -- | 133 | 27.5 | -29 |
| $L3CP_b$ | 318 | 40.5 | 14.0 | C | P | 5 | 8 | 8 | 23 | 115 | 30 | -32.5 |
| L3CN | 301 | 37.4 | 16.4 | C | N | 7 | 8 | 8 | -- | 220 | -- | -41 |
| L3GP | 318 | 40.5 | 14.1 | G | P | 5 | 9 | 10 | 25 | 112 | 27.5 | -35 |
| L3SP | 318 | 40.5 | 14.0 | S | P | 8 | 12 | 12 | 27 | 122 | 30 | -32.5 |
| L3GN | 318 | 40.5 | 14.2 | G | N | 6 | -- | 7 | -- | 170 | -- | -30 |
| L3SN | 318 | 40.5 | 14.2 | S | N | 10 | -- | 11 | -- | 221 | -- | -35 |
| L5IP | 318 | 41.4 | 8.6 | I | P | 21 | 23 | 23 | -- | 236 | 35 | -35 |
| L5IN | 300 | 39.0 | 8.6 | I | N | 22 | -- | 22 | -- | 410 | -- | -30 |
| $L5CP_a$ | 317 | 41.2 | 8.6 | C | P | 9 | 12 | 12 | 19 | 211 | 32.5 | -35 |
| $L5CP_b$ | 317 | 41.2 | 8.6 | C | P | 9 | 12 | 12 | 19 | 214 | 30 | -32.5 |
| L5CN | 318 | 41.4 | 8.6 | C | N | 9 | 13 | 13 | 21 | 378 | 35 | -35 |
| H3IP | 618 | 76.8 | 16.2 | I | P | 18 | 21 | 21 | -- | 78 | 35 | -35 |
| H3IN | 618 | 76.8 | 16.1 | I | N | 18 | -- | 22 | -- | 117 | -- | -35 |
| H3CP | 618 | 76.8 | 16.1 | C | P | 5 | 8 | 9 | 17 | 66 | 32.5 | -35 |
| H3CN | 618 | 76.8 | 16.2 | C | N | 5 | -- | 8 | -- | 104 | -- | -35 |
| H3GP | 618 | 76.8 | 16.0 | G | P | 6 | 9 | 11 | 22 | 75 | 30 | -35 |
| H3SP | 618 | 76.8 | 16.2 | S | P | 9 | 12 | 12 | 22 | 83 | 35 | -35 |

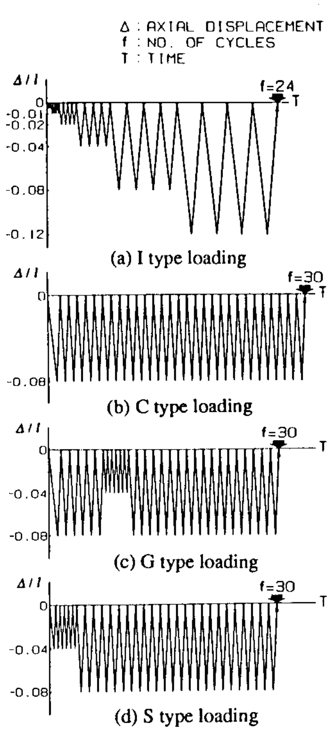


Fig. 1 Loading patterns.

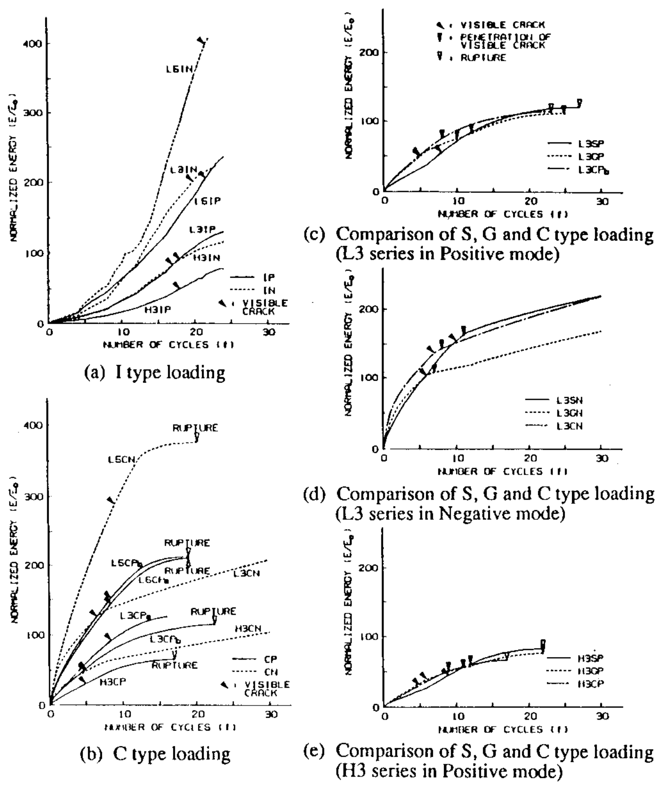


Fig. 2 Comparison of energy dissipation in the course of increasing number of cycles.